

Chapter 8

Nonlinear Control of a Variable Speed Wind Energy Conversion System Based PMSG



Marwa Ayadi and Nabil Derbel

Abstract In this chapter, we present a control system for a variable speed wind turbine based direct-drive permanent magnet synchronous generator. In order to capture the optimal power from the wind and to ensure a maximum efficiency for this system, nonlinear control laws namely backstepping controller and sliding mode controller have been synthesized. Moreover, a blade pitch angle controller has been introduced above rated wind speed to keep the generated power at the designed limit. Finally, to avoid the power fluctuation, the transition between the two control regions has been investigated.

Keywords Wind turbine · PMSG · Blade pitch control · Robust control · Stability

8.1 Introduction

Nowadays, Renewable energy systems receive a great interest in the research community thanks to economic, social and environmental benefits.

In fact, because of the earth greenhouse effects, the oil price increases, the nuclear world security and the rapid growth of the global economy, the renewable energy, which includes geothermal energy, wind energy and photovoltaic energy, etc., has been widely investigated and rapidly developed (Bull 2001).

Wind energy is considered to be the most competitive and the fastest growing renewable energy as it is a clean energy source with an exhaustible supply (Burton et al. 2011).

Several types of wind turbine exist nowadays with variation in the number of blades, the generator type and the control surface. The most prevalent turbine

M. Ayadi (✉) · N. Derbel

National School of Engineering of Sfax (ENIS), University of Sfax, Sfax, Tunisia
e-mail: marwaayadii@yahoo.fr; n.derbel@enis.rnu.tn

existing in the control literature is the 3-blade, horizontal axis wind turbine (HAWT).

For several decades, the wind turbine has been operated at a fixed speed. Despite it has a simple structure and a lower construction and maintenance cost, this type presents some problems as the poor power quality and the low efficiency. Thus, it has been replaced by a variable speed wind turbine (VSWT) to enhance efficiency, reduce audible noise and mechanical stresses (Abulanwar et al. 2016; Burton et al. 2011; Yang et al. 2014b).

For VSWT, the direct– driven permanent magnet synchronous generators (PMSG) are widely used in small and medium-size wind turbine systems. There are several advantages of using PMGs for electrical power generations.

First, they can provide high-reliability and high-efficiency, since there are no copper losses in the rotor circuit and no need for external excitation (Cai et al. 2000).

Second, PMGs with high–power–density are small in size, which reduces the weight and the cost of the wind turbine system (Michalke et al. 2007).

In addition, the wind turbine with a direct-drive PMSG offers the ability to remove the gearbox. According to the statistical data reported in Ribrant and Bertling (2007), failures of gearboxes cause about 19.4% downtime of WTGs. Without gearboxes, the system needs less maintenance and have a higher reliability and a reduced downtime.

The overall configuration of a direct-drive PMSG wind turbine shown in Fig. 8.1. This structure includes a generator control for maintaining the desired rotor speed, a pitch angle control for limiting the output power, a constant DC link control and a grid side inverter control for active and reactive power control.

The main challenge in wind energy conversion system (WECS) control is to extract the optimal accessible power and cope with the nonlinearity of the system. Therefore, in this chapter, we will focus only on analyzing modern nonlinear control techniques for the generator-side to achieve maximum performances.

For the generator side, there are typically two control strategies according to the wind speed velocity.

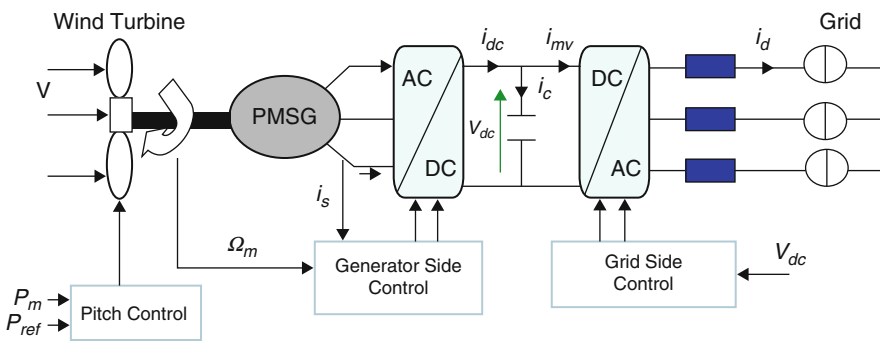


Fig. 8.1 Process structure

In partial load region, the speed controller can continually adjust the speed of the rotor to ensure as much as possible energy yield. Thus, the efficiency of the system will be increased.

For full load zone, the pitch angle regulation is required to keep the generated power constant.

In wind turbine system, control strategies hold a crucial role to enhance the efficiency. Without a good control system, a considerable portion of the produced power is wasted.

Several works of the literature are addressing the issue of controlling the wind turbine system. The simplest techniques are based on PI controllers and the Perturb and Observe algorithm (Kesraoui et al. 2011; Mansour et al. 2011). However, these classical methods show limited performances. Even though neural networks may guarantee a fast response, the performance of control fails along the system variation.

Moreover, fuzzy logic approaches have been widely applied and have presented better effectiveness (Bahraminejad et al. 2014; Jerbi et al. 2009; Simoes et al. 1997), but, the major problems are the strict theoretical analysis and the lack of stability.

A backstepping approach has been studied and developed to the control of the PMSG (Karabacak and Eskinurt 2012; Wang et al. 2013; Yang et al. 2014a). This technique provides a good performance result. Sliding mode control emerges also as a suitable option to deal with such complex system and it has been applied in several works. Lee et al. (2010) propose the sliding mode control scheme to maximize the generated power below the rated wind speed, Results demonstrated by research (Vu et al. 2013; Zhang et al. 2013) involving the use of SMC with PMSG continue to prove the strength of SMC as a viable strategy for effective control of synchronous machines

Although the positive attributes of SMC, the phenomenon known as chattering gives an understandable level of criticism. Because of the nonidealities in switching devices, the response of the system oscillates with high frequencies about the desired reference, known as the sliding surface which leads to low control accuracy and even damages of mechanical parts.

In order to face this undesirable phenomenon, the literature proposes different improvement techniques Such as the approach presented in Kachroo and Tomizuka (1996) which places a boundary layer around the switching surface such that the relay control is replaced by a saturation function. Another class of techniques is based on introducing high order sliding mode algorithms for speed control (Feng et al. 2012; Valenciaga and Puleston 2008). In Evangelista et al. (2013), the speed tracking was achieved using a super-twisting sliding mode control based on Lyapunov techniques.

From this point of view, The main objective of this paper is to study the control algorithms for a variable speed wind turbine based permanent magnet synchronous generator.

In order to achieve a maximum power capture efficiency for the system in safety conditions, a nonlinear control strategy based on backstepping controller and sliding

mode controller has been proposed. Furthermore, a blade pitch angle controller is proposed to enhance system performances in high wind speed region.

The rest of the paper is organized as follow. Section 8.2 presents the system modeling. The control technique applied to the wind system is introduced in Sect. 8.3. The Control below rated wind speed: MPPT zone is presented in Sect. 8.4. Section 8.5 describes the control above rated wind speed (the pitch control). The transition between the two control regions is detailed in Sect. 8.6. Finally, some conclusion remarks are drawn in the last Section.

8.2 Modeling of the Wind Turbine System

8.2.1 Wind Turbine Modeling

Consider a horizontal axis wind turbine (HAWT). The potentially available power by the wind is defined as:

$$P_w = \frac{1}{2}\pi\rho R^2V^3 \quad (8.1)$$

where:

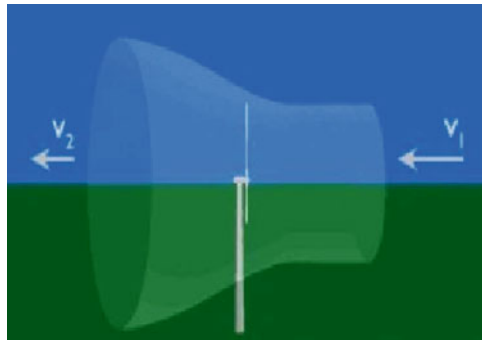
- R denotes the blade radius of the WT(m)
- ρ is the air density (1.25 kg/m in normal atmosphere)
- V is the wind speed (m/s)

However, this expression can only stand if the wind passes through the swept area of the wind turbine.

In 1919, A German physicist Albert Betz state that no more than 59% of the kinetic energy, contained in a steam tube that shares the same cross-section as the disc, can be converted to useful works.

Figure 8.2 presents a schematic of fluid flow which helps to contextualize the statement.

Fig. 8.2 Schematic of fluid flow through a wind turbine



Thus, a power coefficient term is introduced and can be understood as:

$$C_p = \frac{\text{mechanical power captured by the wind turbine}}{\text{maximum power available in the wind}} \tag{8.2}$$

C_p represents the performance of the wind turbine. It depends on the tip-speed ratio (TSR) λ and the pitch angle β which is the angle between the orientation of the blade and the wind velocity vector:

$$C_p(\lambda, \beta) = 0.22 \left(\frac{116}{\lambda_i} - 0.4\beta - 5 \right) e^{\frac{-12.5}{\lambda_i}}$$

$$\frac{1}{\lambda_i} = \frac{1}{\lambda + 0.08\beta} - \frac{0.035}{\beta^3 + 1} \tag{8.3}$$

with

$$\lambda = \frac{\Omega_t R}{V} \tag{8.4}$$

where Ω_t is the turbine speed

The nonlinear relation between C_p , λ and β is presented in Fig. 8.3.

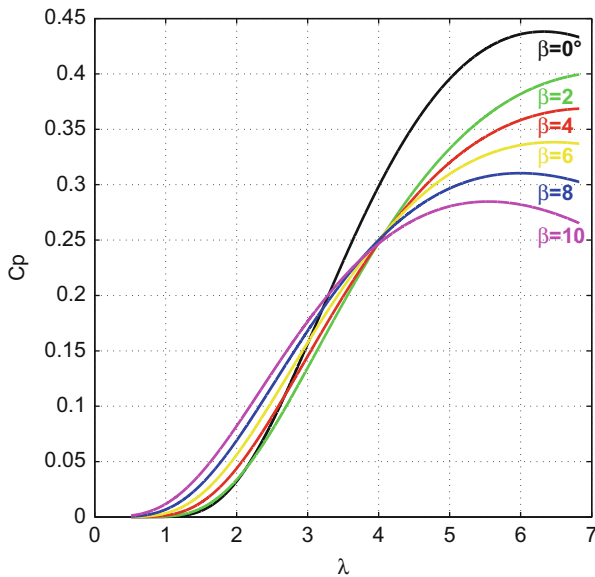


Fig. 8.3 Aerodynamic power coefficient variation C_p against the speed ratio λ and the pitch angle β

It is obvious that C_p is maximised when $\beta = 0$ and it decreases with the increase of β . For a constant pitch angle, there is a unique peak of the curve corresponding to C_{pmax} .

The aerodynamic torque is given by:

$$T_m = \frac{P_m}{\Omega_t} = \frac{1}{2} \pi \rho C_p(\lambda, \beta) \frac{R^2 V^3}{\Omega_t} \quad (8.5)$$

8.2.2 PMSG Modeling

The mathematical model of the PMSG in the d-q reference is Kim et al. (2010):

$$\begin{cases} U_d = R_s I_d + L_d \frac{di_d}{dt} - \Omega_e \Phi_q \\ U_q = R_s I_q + L_q \frac{di_q}{dt} + \Omega_e \Phi_d \end{cases} \quad (8.6)$$

where R_s is the stator resistance. Φ_d and Φ_q are the d and q axis flux linkage, respectively:

$$\begin{aligned} \Phi_d &= L_d I_d + \Phi_m \\ \Phi_q &= L_q I_q \end{aligned} \quad (8.7)$$

Furthermore, consider $L_q = L_d = L_s$ denotes the inductance of the stator (a PMSG with a nonsalient pole is considered in this study).

8.3 Control Technique

Wind Turbine systems present intense nonlinearities, and are subjected to disturbances and parameter uncertainties. Such factors transform their control to a hard task.

Therefore, a high level control is often required in order to ensure a certain convergence of the system to the requested state condition and to operate at maximum power coefficient over a wide range of wind speeds.

In fact, wind turbines should be driven differently according to the speed of the wind.

Therefore, the WT generator needs to be controlled to operate in three different modes as shown in Fig. 8.4.

- **Parking Mode (I):** The wind speed is lower than the cut-in speed which is (2 m/s) in this system, the wind turbine stays in a parking status and does not rotate.

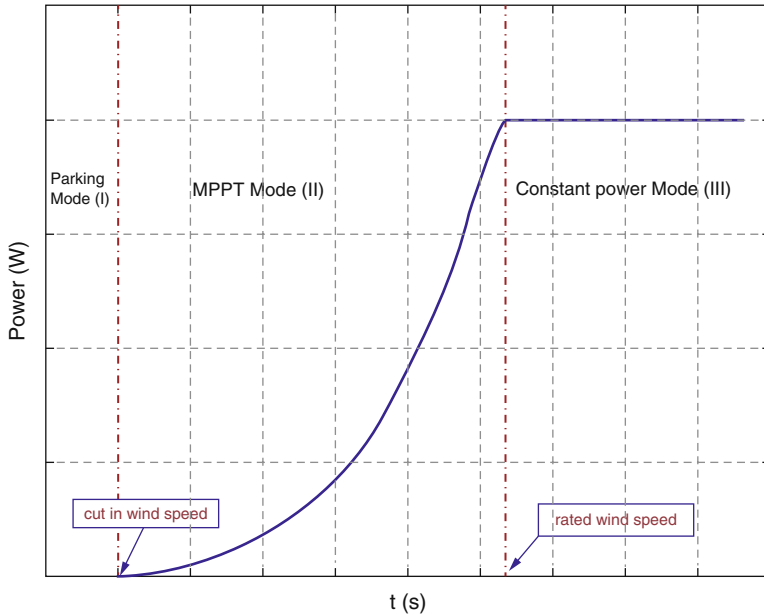


Fig. 8.4 Power versus wind speed characteristic

- MPPT (Maximum Power Point Tracking) mode (II): The system starts to work and generates electrical power. The MPPT is applied until arrived to the rated wind speed, (12.7 m/s), for this case-study system. The blade angle is usually controlled at zero degree to maximize the wind energy capture.
- Constant power Mode (III): It is necessary to control the extracted power above rated wind value by adjusting properly the blade pitch angle of the wind turbine to keep the power at constant power region, as its name implies.

8.4 Control Below Rated Wind Speed: MPPT Zone

In this region, the wind speed is below the rated value. The objective of the controller is to maximize the wind energy capture and to achieve the Maximum Point Power Tracking (MPPT). For that, The tip speed ratio λ is set to its optimal value λ_{opt} which contributes to the power coefficient peak C_{pmax} . Therefore, the optimum rotor speed of the Wind turbine can be written as follows:

$$\Omega_{opt} = \frac{\lambda_{opt} v}{R} \tag{8.8}$$

Thus, the maximum power output of the wind turbine can be expressed as:

$$P_{max} = k_{opt} \Omega_{opt}^3 \quad (8.9)$$

$$k_{opt} = \frac{1}{2} C_{pmax} \rho \pi R^2 \left(\frac{R}{\lambda_{opt}} \right)^3$$

In addition, to achieve the MPPT operation mode, the pitch angle is kept at zero degree to ensure a high efficiency of energy capture.

The optimum rotor speed given in Eq. (8.8) is considered as the speed reference of the PMSG. Consequently, by using a robust control technique the generator speed will reach its reference value in the static state, and then the MPPT control is achieved.

In this work, the control system proposed to command the wind turbine generator is the Field Oriented Control (FOC), which controls the torque indirectly by adjusting the stator currents. In this method, the torque angle is maintained at 90° . The d-axis current is set to zero and then the stator current has only the q-axis component. Thus, the torque depends only on the q-axis stator current. This technique removes current cross coupling between the d and q axes components.

Based on the FOC technique, different controller design have been investigated in this work to the PMSG to optimize the wind turbine power output.

- Proportional Integral (PI) control
- backstepping control
- Sliding mode control

Remark 1 For the control design, the following assumptions are required:

Assumption 1 Variables i_q , i_d and Ω are available.

Assumption 2 The reference speed Ω_{ref} is determined referring to the MPPT algorithm.

Assumption 3 The d-axis reference current should be equal to zero $i_d = 0$.

8.4.1 Vector Control Based PI Controller

8.4.1.1 Controller Design

This technique is the most commonly applied algorithm for the PMSG control (Ayadi and Derbel 2017). It involves two control loops:

- two inner current loops are used to adjust the generator currents i_d and i_q allowing the control of the flux and the torque, respectively.
- an external mechanical loop in order to ensure the speed regulation.

Then, to improve the dynamic response, compensation voltage, ΔU_q and ΔU_d are added into the control law.

$$\begin{aligned}\Delta U_d &= \Omega_e i_q L_s \\ \Delta U_q &= \Omega_e i_q L_s + \Omega_e \Phi_m\end{aligned}\quad (8.10)$$

- d-axis current controller design

The control of this component aims to keep the stator flux constant. Its reference value is set to zero.

$$\frac{i_d}{U_d} = \frac{\frac{1}{R_s}}{1 + s \frac{L_d}{R_s}} \quad (8.11)$$

The PI transfer's function is:

$$G(s) = k_d \left(\frac{1 + \tau_d s}{\tau_d s} \right) \quad (8.12)$$

Based on the compensation pole method, the synthesis of this PI can be determined $\tau_d = \frac{L_d}{R_s}$, $K_d = \frac{R_s^2}{L_d}$, and the closed loop transfer function between the actual and the desired direct current is:

$$F_d(s) = \frac{1}{1 + s \frac{L_s}{R_s}} \quad (8.13)$$

- q-axis current controller design

The control of the quadrature current i_q affects directly the electromagnetic torque. The reference value of i_q is determined from the speed control loop. The control law is implemented in the same way as the d-axis current controller yielding: $\tau_q = \frac{L_s}{R_s}$ and $K_q = \frac{R_s^2}{L_s}$.

- Speed control loop

The reference value of this loop is the optimal speed Ω_{opt} determined based on the MPPT strategy Eq. (8.8). The transfer function between Ω_r and i_q is given by:

$$\frac{i_q}{\Omega_r} = \frac{\frac{3}{2} p \Phi_m}{f + s J} \quad (8.14)$$

Table 8.1 Turbine and PMSG parameters

Wind turbine parameters	PMSG parameters
3 blades	$P_{nom} = 25 \text{ KW}$
Variable speed	$R_s = 0.82 \text{ m}$
$R = 4.5 \text{ m}$	$L_{sd} = L_{sq} = 15.1 \text{ mH}$
$C_{pmax} = 0.42$	$\phi = 0.5 \text{ Wb}$
$J_{tot} = 99 \text{ e-4}$	$f = 1\text{e-3}$
$\rho = 1.225 \text{ kg/m}$	$p = 4$

The PI transfer's function is:

$$G_{\Omega}(s) = k_{\Omega} \left(\frac{1 + \tau_{\Omega}s}{\tau_{\Omega}s} \right) \quad (8.15)$$

Thus, the closed-loop transfer function is:

$$F_{\Omega}(s) = \frac{1 + \tau_{\Omega}s}{1 + (\tau_{\Omega} + \frac{f}{\frac{3}{2}p\phi_m K_{\Omega}})s + \frac{J}{\frac{3}{2}p\phi_m K_{\Omega}}s^2} \quad (8.16)$$

The output of the PI represents the quadrature reference current \bar{i}_q .

8.4.1.2 Simulation Results

Results have been presented, using numerical simulations carried under the Matlab-SIMULINK tool to test the control strategy and to evaluate the performance of the system.

Characteristics of the turbine and the Permeant Magnetic Synchronous Machine are presented in Table. 8.1.

System simulation has been performed considering an aleatory wind profile to evaluate the behavior of the system similar to real conditions.

As shown in Fig. 8.4, for different regions of the wind speed, there is a specific control strategy. Therefore in this part, The wind speed will be limited to (11.5 m/s) as we are interested in the control below rated wind speed region(II).

- Figure 8.5a presents the wind speed profile.
- Figure 8.5b shows that the power coefficient C_p is maintained close to its maximum value $C_{pmax} = 0.41$. Thus, the Maximum Power Point Tracking MPPT has been achieved.
- The system response under PI is shown in Fig. 8.6.

Figure 8.6a shows the rotational speed response. It converges to its reference track which is supplied from the Maximum Power Point Tracking (MPPT) controller. Figure 8.6b presents the rotational speed error which exceeds the 0.2(rad/s). The direct and the quadrature currents are shown in Fig. 8.6c, e respectively. It is obvious from Fig. 8.6d, f that current errors present a considerable distorted values due to the nonlinear characteristics of the system

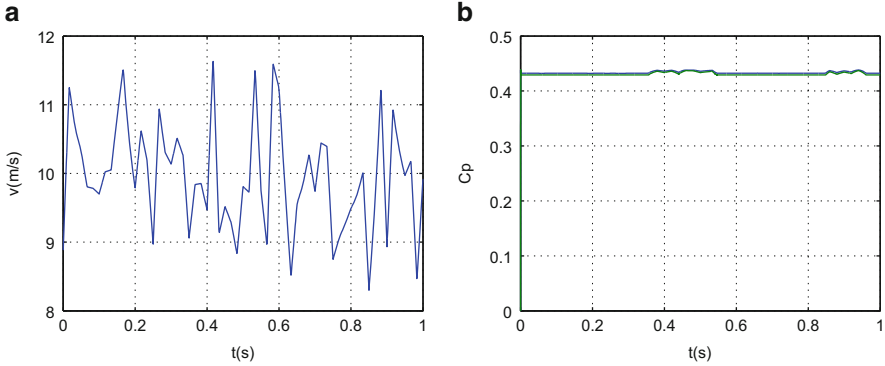


Fig. 8.5 wind speed profile

This control laws gives good dynamic response of the speed tracking and remarkable rejection of disturbances.

However, it should be noted that it is better to minimize as possible the tracking error, hence we propose two non-linear regulators namely the backstepping control and the sliding mode control in the sequel.

8.4.2 Backstepping Controller

8.4.2.1 Controller Design

This control approach is designed in such a way it keeps the same general structure of the vector control while ensuring at the same time the regulation and the limitation of the currents. The objective of the nonlinear backstepping controller is to track the speed of PMSG with the choice of appropriate regulated variables (Ayadi and Derbel 2017). Based on the PMSG model given in Eq. (8.6), The control design can be determined by following three steps as shown in Fig. 8.7.

- *Step 1: Control design based on rotational speed dynamics:*

The speed error is:

$$e_{\Omega} = \bar{\Omega}_r - \Omega_r \tag{8.17}$$

The error dynamics derived can be obtained as:

$$\dot{e}_{\Omega} = \dot{\bar{\Omega}}_r - \frac{T_m}{J} + \frac{3p}{2J} \Phi_m i_q + \frac{B}{J} \Omega_r \tag{8.18}$$

Consider the following Lyapunov function candidate:

$$V_{\Omega} = \frac{1}{2} e_{\Omega}^2 \tag{8.19}$$

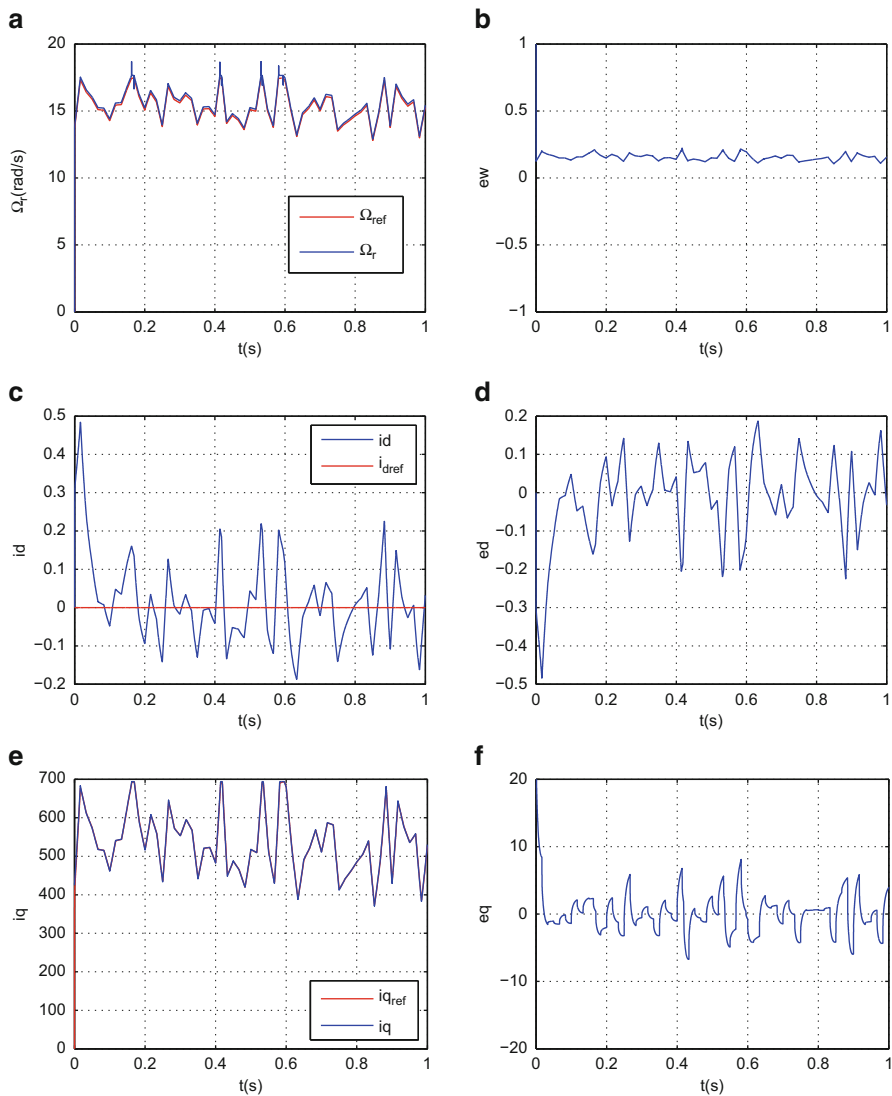


Fig. 8.6 Simulation results of the FOC based PI controller. (a): rotational speed, (b): Speed error, (c):direct current, (d): direct current error, (e):quadrature current, (f):quadrature current error

Its derivative is:

$$\dot{V}_{\Omega} = e_{\Omega} \dot{e}_{\Omega} = e_{\Omega} \left(\dot{\Omega}_r - \frac{T_m}{J} + \frac{3p}{2J} \Phi_m i_q + \frac{B}{J} \Omega_r \right) \quad (8.20)$$

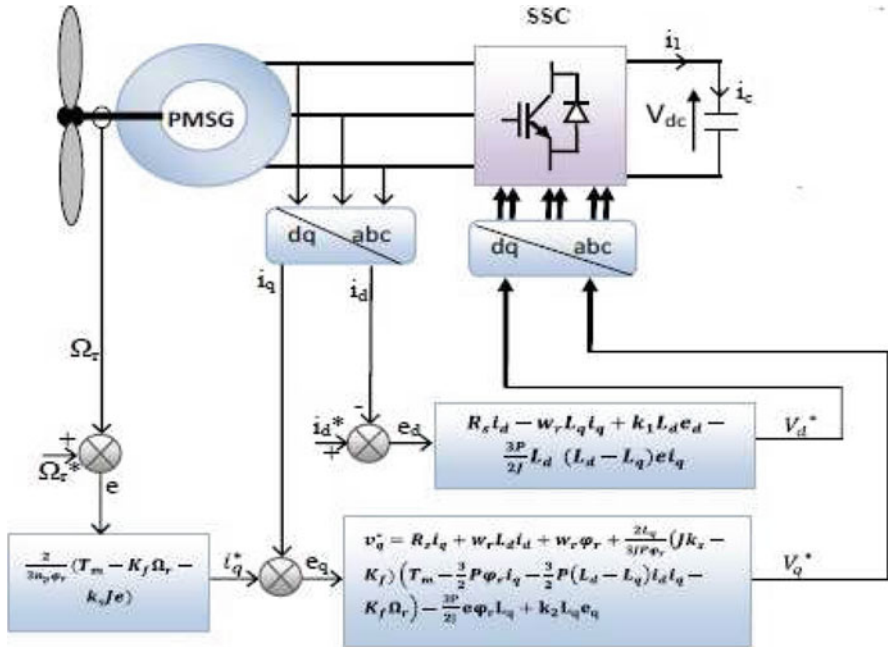


Fig. 8.7 Internal structure of the backstepping controller block

The direct and quadrature current i_d and i_q are chosen as virtual control elements:

$$\begin{cases} \bar{i}_d = 0 \\ \bar{i}_q = \frac{2J}{3p\Phi_m} \left(-\dot{\Omega}_r + \frac{T_m}{J} - \frac{B}{J}\Omega_r - K_\Omega e_\Omega \right) \end{cases} \quad (8.21)$$

where $K_\Omega > 0$

Thus:

$$\dot{V}_\Omega = -K_\Omega e_\Omega^2 \quad (8.22)$$

• Step 2: Current components control design

The current error can be determined as:

$$\begin{aligned} e_d &= \bar{i}_d - i_d \\ e_q &= \bar{i}_q - i_q \end{aligned} \quad (8.23)$$

The error dynamics derived from Eqs. (8.18), (8.21) and (8.23) are:

$$\begin{aligned}\dot{e}_d &= \frac{R_s}{L_s}i_d - pi_q\Omega_r - \frac{1}{L_s}U_d \\ \dot{e}_q &= \frac{2J}{3p\Phi_m} \left(-\ddot{\Omega}_r - \frac{B}{J}\dot{\Omega}_r - K_\Omega e_\Omega \right) + \frac{R_s}{L_s}i_q + p \left(i_d + \frac{\Phi_m}{L_s} \right) \Omega_r - \frac{1}{L_s}U_q \\ \dot{e}_\Omega &= -\frac{3p\Phi_m}{2J}e_q - K_\Omega e_\Omega\end{aligned}$$

- *Step 3: Control laws design*

The Lyapunov function is determined as:

$$V_2 = \frac{1}{2}(e_\Omega^2 + e_d^2 + e_q^2) \quad (8.24)$$

Its time derivative is:

$$\begin{aligned}\dot{V}_2 &= (e_\Omega \dot{e}_\Omega + e_d \dot{e}_d + e_q \dot{e}_q) - K_\Omega e_\Omega^2 - K_d e_d^2 - K_q e_q^2 - e_\Omega \frac{3p\Phi_m}{2J}e_q \\ &+ e_q \left[\frac{2J}{3p\Phi_m} \left(-\ddot{\Omega}_r - \frac{B}{J}\dot{\Omega}_r - K_\Omega e_\Omega \right) + \frac{R_s}{L_s}i_q + p \left(i_d + \frac{\Phi_m}{L_s} \right) \Omega_r \right. \\ &\quad \left. - \frac{1}{L_s}U_q + K_q e_q \right] + e_d \left[\frac{R_s}{L_s}i_d - pi_q\Omega_r - \frac{1}{L_s}U_d + K_d e_d \right] \quad (8.25)\end{aligned}$$

The control inputs which stabilize The current tracking errors dynamics are:

$$\bar{v}_d = R_s i_d - L_s pi_q \Omega_r + L_s K_d e_d \quad (8.26)$$

$$\bar{v}_q = \frac{2JL_s}{3p\Phi_m} \left(-\ddot{\Omega}_r - \frac{B}{J}\dot{\Omega}_r - K_\Omega e_\Omega \right) + R_s i_q + p(i_d L_s + \Phi_m)\Omega_r + K_d L_s e_d$$

This choice yields:

$$\dot{V}_2 = -K_\Omega e_\Omega^2 - K_d e_d^2 - K_q e_q^2 \leq 0 \quad (8.27)$$

where K_d and K_q are positive gains.

8.4.2.2 Simulation Results

The same wind speed profile is applied in this part with varying degrees of wind speed between (8 m/s) and (11.5 m/s).

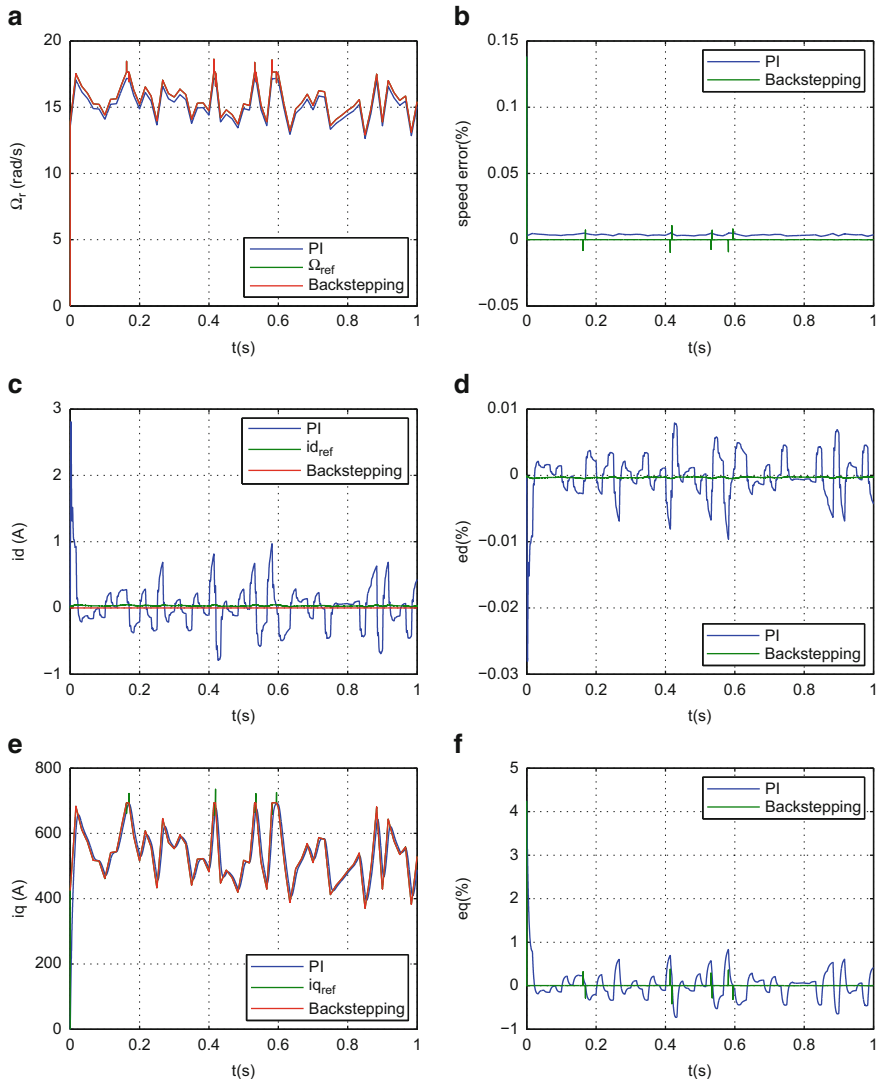


Fig. 8.8 Simulation results

- The system response under PI controller and nonlinear backstepping control has been presented in Fig. 8.8.

Figure 8.8a presents the rotational speed response which converges perfectly to its reference track. Figure 8.8b shows the speed error. Its is neglected for the backstepping control compared to PI controller. Figures 8.8c, e illustrate the direct and the quadrature currents, respectively. The evolution of the currents errors (Fig. 8.8d, f) shows that the backstepping control has a good dynamic response.

8.4.3 Sliding Mode Control

8.4.3.1 Controller Design

The sliding mode control has proved to be an efficient technique able to cope with aforementioned complex characteristics. In this context, this technique is applied in this section to design a robust controller for nonlinear multi-input multi-output permanent magnet synchronous generator based WECS. The controller design is ensured by the following steps.

1. *Sliding surfaces:*

Based on the system model, the sliding surfaces are to be defined as:

$$S_d(t) = e_d(t) + \lambda_1 \int e_d(t) dt \quad (8.28)$$

$$S_q(t) = e_q(t) + \lambda_2 \int e_q(t) dt \quad (8.29)$$

$$S_{\Omega_r}(t) = e_{\Omega_r}(t) + \lambda_3 \int e_{\Omega_r}(t) dt \quad (8.30)$$

where $e_d(t) = i_d(t) - i_{dref}(t)$, $e_q(t) = i_q(t) - i_{qref}(t)$ and $e_{\Omega_r}(t) = \Omega_r(t) - \Omega_{rref}(t)$.

The integral action has been included to overcome the state error and to improve the sliding surface where $\lambda_1, \lambda_2, \lambda_3$ are the integral gains.

2. *Reachability:*

The reachability condition for Eqs. (8.28), (8.29) and (8.30) are defined respectively as:

$$S_d(t) \dot{S}_d(t) < 0 \quad (8.31)$$

$$S_q(t) \dot{S}_q(t) < 0 \quad (8.32)$$

$$S_{\Omega_r}(t) \dot{S}_{\Omega_r}(t) < 0 \quad (8.33)$$

3. *d-axis current control design*

The control of i_d component current aims to keep the stator flux constant. Its reference value is set to zero.

From Eq. (8.21), the inequality Eq. (8.31) can be rewritten as:

$$S_d(t) \left[\left(\lambda_1 - \frac{R_s}{L_s} \right) i_d + p i_q \Omega_r + \frac{1}{L_s} U_d \right] < 0 \quad (8.34)$$

The d-axis control law is given by:

$$U_d(t) = U_{deq}(t) + \Delta U_d \quad (8.35)$$

with the equivalent control U_{deq} is:

$$U_{deq}(t) = (R_s - \lambda_1 L_s) i_d - p i_q \Omega_r L_s \quad (8.36)$$

The switching control ΔU_d is defined as:

$$\Delta U_d = K_d \text{sign}[S_d(t)] \quad (8.37)$$

where K_d is a positive constant

4. **q-axis current control design**

Based on the system model and following the similar method, Eq. (8.32) becomes:

$$S_q(t) \left[\left(\lambda_2 + \frac{R_s}{L_s} \right) i_q - p \left(i_d + \frac{\Phi_m}{L_s} \right) \Omega_r + \frac{1}{L_s} U_q + \lambda_2 i_{qref} \right] < 0$$

Denoting the control law as:

$$U_q(t) = U_{qeq}(t) + \Delta U_q \quad (8.38)$$

The equivalent control can be given as:

$$U_{qeq} = (R_s + L_s \lambda_2) i_q + p(L_s i_d + \phi_m) \Omega_r - \lambda_2 L_s i_{qref} - L_s \frac{di_{qref}}{dt} \quad (8.39)$$

where i_{qref} is a dynamic value that will be determined as a resulting output of the rotational speed control.

The switching portion of the $U_q(t)$ can be expressed by:

$$\Delta U_q = K_q \text{sign}[S_q(t)] \quad (8.40)$$

where K_q is a positive constant

5. **Rotational speed dynamics control**

This controller should ensure that the rotational speed. It is driven to its reference determined by the MPPT algorithm. Considering the rotational speed motion equation, the inequality Eq. (8.33) becomes:

$$S_{\Omega_r}(t) \left[\frac{T_m}{J} - \frac{3}{2J} p \Phi_m i_q + \left(\lambda_3 - \frac{B}{J} \right) \Omega_r - \lambda_3 \Omega_{ref} \right] < 0 \quad (8.41)$$

The control variable for the rotational speed controller is the quadrature axis reference current which is designed as:

$$i_{qref}(t) = i_{qeq.ref}(t) + \Delta i_{qref} \quad (8.42)$$

The equivalent control law is given as:

$$i_{qref} = \frac{2}{3p\phi_m} [T_m + (\lambda_3 J - B)\Omega_r - \lambda_3 \Omega_{ref}] \quad (8.43)$$

It then follows that:

$$\Delta i_{qref} = K_{iq} \text{sign}[S_{\Omega_r}(t)] \quad (8.44)$$

where K_{iq} is a positive constant

In order to reduce the chattering effect, a smooth control discontinuity is introduced around the switching surface. The sign $[S(t)]$ is replaced by $\text{sat}[S(t), \Delta]$ which can be expressed as:

$$\text{sat}[S(t)] = \begin{cases} \frac{S(t)}{\Delta} & \text{if } |S(t)| \leq \Delta \\ \text{sign}(S(t)) & \text{otherwise} \end{cases} \quad (8.45)$$

where Δ is the boundary layer thickness.

8.4.3.2 Simulation Results

The system response under the Sliding Mode concept has been presented in Fig. 8.9.

The rotational speed $\Omega_r(t)$ is shown in Fig. 8.9a. The second result shown is that of $i_d(t)$. As it can be seen by Fig. 8.9c, the d-axis current accurately tracks the reference value $i_{dref} = 0$. Figure 8.9e. shows the actual value of $i_q(t)$, accurately tracking the defined reference.

8.5 Control Above Rated Wind Speed: Pitch Control

8.5.1 Introduction

The key part of a variable-speed wind turbine is the pitch system. Its main purpose is to keep the generated power constant above the rated wind speed.

In fact, when the wind speed becomes larger than the rated value and the MPPT algorithm is still applied, the power generated by the system will exceed the optimal power if the blade angle β stays fixed at zero degrees.

This will make the power devices and the generator work in a higher zone than optimum output, which is harmful to the mechanical system if sustained for a period of time.

Based on this concern, a control system for the regulation of the pitch angle according to different wind conditions is required for the wind turbine.

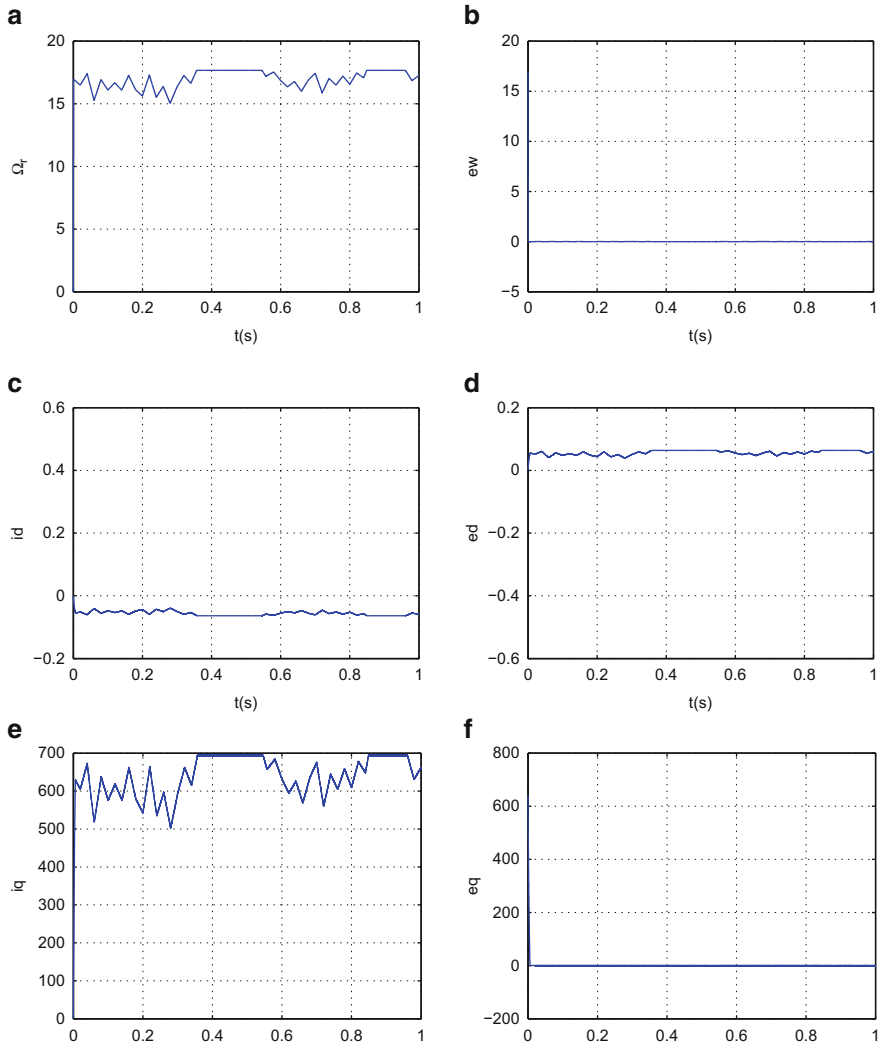


Fig. 8.9 Simulation results of the Sliding mode strategy

Small changes in the blade angle can have dramatic effects on the output power. The advantages of the pitch control system might be summarized as follows:

1. Optimize the output power of the wind turbine. Indeed, to give the maximum power in partial load region, the pitch setting should be at its optimum value
2. Prevent input mechanical power to exceed the design limits. This controller provides a good regulation of the aerodynamic power and the loads produced by the rotor.

3. Minimize the fatigue loads of the turbine mechanical components. The design of the controller must take into account the load.

Thus, the blade pitch angle control should have a good dynamic quality and a strong robustness.

Several works on pitch control have been done to improve the quality of the generated power. For example, a gain scheduling controller, proposed in Lescher et al. (2005), changes the controller gain with the variation of the wind speed. However, the practical implementation of the gain scheduling is very difficult because the wind speed is usually measured on the tower and does not represent the wind speed at the turbine plant. Disturbance accommodating control (DAC) has been developed in Stol et al. (2000, 2003), but it presents a large estimation error when the system operates far away from the rated wind speed. H_∞ controllers for blade pitch control and electromagnetic torque control have been used in Rocha et al. (2003). However, this controller has not been experienced on a nonlinear turbine model.

Based on the analysis of the above studies, we propose two types of controllers to solve the variable pitch control problem of a direct-drive PMSG wind turbine (Ayadi et al. 2017):

- Pitch Control based on a Proportional Integrator controller
- Pitch Control based on a Sliding Mode controller

8.5.2 System Description

The blade pitch control system is the key part of a variable speed wind turbine. It acts directly on the system responses for different wind speed zones (Fig. 8.10).

To regulate the blade angle, the power deviation from its reference value is used.

An electromechanical system called actuator is then used to put the blade angle into the desired position. It can be modeled as a first-order system as Hwas and Katebi (2012):

Fig. 8.10 Schematic illustration of the Kinematics of the WT



$$G(s) = \frac{k_0}{1 + \tau s} \quad (8.46)$$

k_0 is the proportional gain and τ is the time constant.

According to industrial recommendations, it is necessary to include a pitch rate adjusted to $10^\circ/s$

8.6 Transition Between the Two Control Regions

8.6.1 Switched Wind Turbine System

Variable speed wind turbines operate within a large range of wind speeds. During the power generation and depending on the prevailing wind speed, the wind turbine switches between two operation modes as shown in Fig. 8.4: the low wind speed region (also called Region II) where the control objective is to capture the maximum power from the wind and the high wind speed region (also called Region III) where the control aim is to limit the output power to the required power.

The control of a variable speed wind turbine is usually achieved based on two distinct control laws for Regions (II) and (III), respectively. The switching or called also transition between these two regions cause undesirable effects such as vibrations in drive train, tower and blades (Pao and Johnson 2009) which cause system fatigue and premature failure.

Therefore, it is necessary to develop a control algorithm to smooth out the undesirable effects of the switching actions and also to stabilize the switching operation.

The synthesis of the blade angle controller is divided typically into two zones according to the wind speed value:

- Partial load zone: $v < v_{ref} \rightarrow \beta = \beta_{ref} = 0$
- Full load zone: $v \geq v_{ref} \rightarrow \beta$ changes with the wind variation to keep $P = P_{opt}$

There are usually two controllers for the variable-speed wind turbines which are cross-coupled each other, shown as in Fig. 8.11.

In order to smooth the wind power fluctuations in the intermediate zone, a fuzzy logic controller has been investigated.

8.6.2 Simulation Results

To validate the stability of the system when it switches between Region (II) and Region (III) modes, simulations have been performed on a system with the following conditions:

1. Maximum Power Coefficient (C_{pmax}) = 0.4109

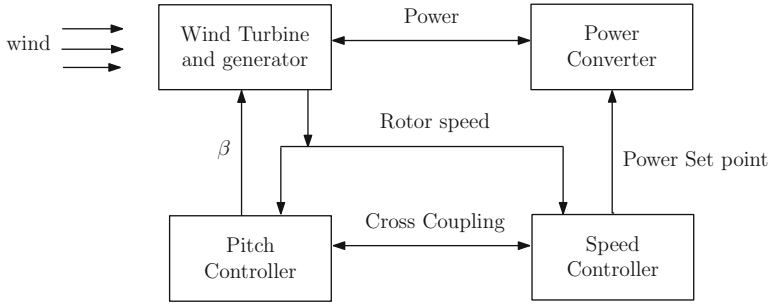


Fig. 8.11 Structure of a model of variable-speed wind turbine

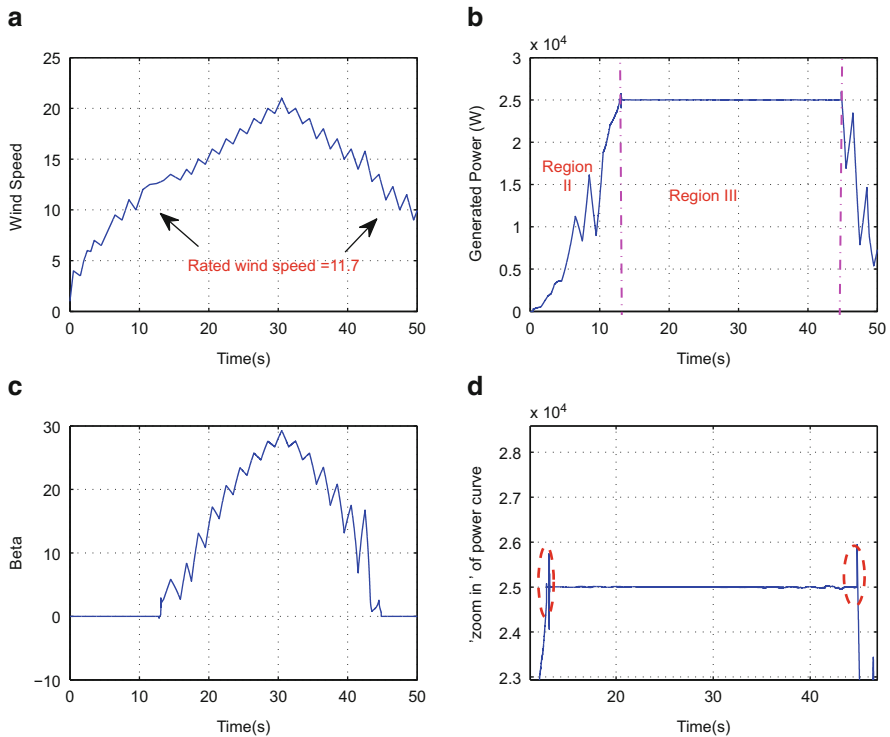


Fig. 8.12 Simulation results in full range of operation

2. Rated wind speed $V_m = 11.7$
3. Nominal Demand Power (P_{max}) = 2.5 kW

Figure 8.12a presents the wind speed profile which involves the two operational areas, i.e., the low wind speed area ($V < 11.7$ m/s) and the high wind speed area ($V \geq 11.7$ m/s).

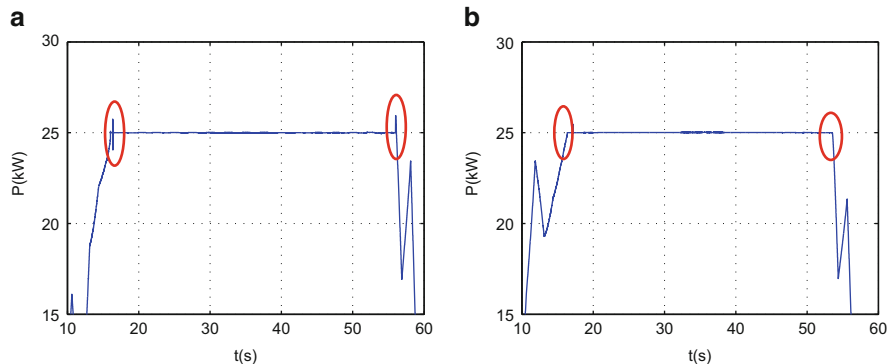


Fig. 8.13 Simulation in the transition region

The power characteristic is shown in Fig. 8.13b. The turbine starts operating when the wind speed exceeds cut-in wind speed 3 m/s. In this region (II), The MPPT algorithm and the torque control come into action with a constant pitch angle.

When the wind speed exceeds its nominal value (region III), the control objective shifts from maximizing the power capture to regulate the power to the turbine rated output.

Figure 8.12c shows the pitch angle variation. Below the rated wind speed the blade pitch angle is set at 0. It is the optimal value that allows the turbine to extract the maximum energy from the incident wind. Otherwise, the pitch control is active: the angle changes with the variations of the wind to avoid over rated power.

Figure 8.12d presents a zoomed in section of Fig. 8.13b. It is obvious that Between the high and the low wind speed region, the curve of the output power presents a noticeable fluctuation caused by the transition between the two regions which causes system fatigue and premature failure.

As a solution, a fuzzy logic controller has been applied with the aim of smoothing the wind power fluctuations in the intermediate zone. Figure 8.13a presents the wind speed profile with varying degrees. Figure 8.13b presents the power coefficient C_p . It can be observed that the C_p curve is maintained close to its maximum value $C_{pmax} = 0.41$ which proves that the MPPT has been achieved. In region (III) as the power coefficient depends on the blade pitch angle, it varies with the blade variations.

Figure 8.13c presents the generated power for the 2 control zones: It is remarkable that the fluctuation between the intermediate zone has been eliminated. The wind speed moves from zone to another fluently. The variation of the pitch angle is illustrated in Fig. 8.13d. The pitch angle controller shows a perfect capability of giving to the actuator the right angle demand in different wind speed zones. The rotational speed is presented in Fig. 8.13e, (in region II) the speed is varying to optimal power extraction, overrated wind speed, the speed control input is considered as its maximum value.

8.7 Conclusion

This chapter discusses the control systems used for a variable speed wind turbine equipped with PMSG. In the first part, a control algorithm has been synthesized to extract the maximum of the power based on two nonlinear control techniques namely the backstepping controller and the sliding mode controller. Comparative studies between these algorithms have been presented. Then, above rated wind speed, a pitch angle regulation has been investigated to keep the generated power at the designed limit.

Finally, the transition between the two control regions has been discussed to avoid the power fluctuation.

References

- Abulanwar, S., Hu, W., Chen, Z., & Iov, F. (2016). Adaptive voltage control strategy for variable-speed wind turbine connected to a weak network. *IET Renewable Power Generation*, 10(2), 238–249.
- Ayadi, M., & Derbel, N. (2017). Nonlinear adaptive backstepping control for variable-speed wind energy conversion system-based permanent magnet synchronous generator. *The International Journal of Advanced Manufacturing Technology*, 92(1–4), 39–46.
- Ayadi, M., Ben Salem, F., & Derbel, N. (2017). Power control of a variable speed wind turbine based on direct torque control of a permanent magnet synchronous generator. *International Journal of Digital Signals and Smart Systems*, 1(3), 204–223.
- Bahraminejad, B., Iranpour, M. R., & Esfandiari, E. (2014). Pitch control of wind turbines using IT2FL controller versus T1FL controller. *International Journal of Renewable Energy Research (IJRER)*, 4(4), 1065–1077.
- Bull, S. R. (2001). Renewable energy today and tomorrow. *Proceedings of the IEEE*, 89(8), 1216–1226.
- Burton, T., Jenkins, N., Sharpe, D., & Bossanyi, E. (2011). *Wind energy handbook* (2nd ed.). John Wiley & Sons.
- Cai, W., Fulton, D., & Reichert, K. (2000). Design of permanent magnet motors with low torque ripples: A review. *International Conference on Electrical Machines* (pp. 1384–1388).
- Evangelista, C., Puleston, P., Valenciaga, F., & Fridman, L. M. (2013). Lyapunov-designed super-twisting sliding mode control for wind energy conversion optimization. *IEEE Transactions on Industrial Electronics*, 60(2), 538–545.
- Feng, Y., Chen, B., Yu, X., & Yang, Y. (2012). Terminal sliding mode control of induction generator for wind energy conversion systems. In *IECON 2012: 38th Annual Conference on IEEE Industrial Electronics Society* (pp. 4741–4746). IEEE.
- Hwas, A., & Katebi, R. (2012). Wind turbine control using PI pitch angle controller. *IFAC Proceedings Volumes*, 45(3), 241–246.
- Jerbi, L., Krichen, L., & Ouali, A. (2009). A fuzzy logic supervisor for active and reactive power control of a variable speed wind energy conversion system associated to a flywheel storage system. *Electric Power Systems Research*, 79(6), 919–925.
- Kachroo, P., & Tomizuka, M. (1996). Chattering reduction and error convergence in the sliding-mode control of a class of nonlinear systems. *IEEE Transactions on Automatic Control*, 41(7), 1063–1068.

- Karabacak, M., & Eskikurt, H. I. (2012). Design, modelling and simulation of a new nonlinear and full adaptive backstepping speed tracking controller for uncertain PMSM. *Applied Mathematical Modelling*, 36(11), 5199–5213.
- Kesraoui, M., Korichi, N., & Belkadi, A. (2011). Maximum power point tracker of wind energy conversion system. *Renewable Energy*, 36(10), 2655–2662.
- Kim, H.-W., Kim, S.-S., & Ko, H.-S. (2010). Modeling and control of PMSG-based variable-speed wind turbine. *Electric Power Systems Research*, 80(1), 46–52.
- Lee, S.-H., Joo, Y.-J., Back, J., & Seo, J. H. (2010). Sliding mode controller for torque and pitch control of wind power system based on pmsg. In *IEEE International Conference on Control Automation and Systems (ICCAS)* (pp. 1079–1084).
- Lescher, F., Zhao, J. Y., & Borne, P. (2005). Robust gain scheduling controller for pitch regulated variable speed wind turbine. *Studies in Informatics and Control*, 14(4), 299.
- Mansour, M., Mansouri, M., & Mmimouni, M. (2011). Study and control of a variable-speed wind-energy system connected to the grid. *International Journal of Renewable Energy Research*, 1(2), 96–104.
- Michalke, G., Hansen, A. D., & Hartkopf, T. (2007). Control strategy of a variable speed wind turbine with multipole permanent magnet synchronous generator. In *European Wind Energy Conference and Exhibition*.
- Pao, L. Y. & Johnson, K. E. (2009). A tutorial on the dynamics and control of wind turbines and wind farms. In *IEEE American Control Conference, ACC'09* (pp. 2076–2089).
- Ribrant, J., & Bertling, L. (2007). Survey of failures in wind power systems with focus on swedish wind power plants during 1997–2005. In *Power Engineering Society General Meeting, IEEE*, (pp. 1–8). IEEE.
- Rocha, R., Filho, L. S. M. (2003). A multivariable H_∞ control for wind energy conversion system. In *IEEE Conference on Control Applications, CCA* (pp. 206–211).
- Simoes, M. G., Bose, B. K., Spiegel, R. J. (1997). Fuzzy logic based intelligent control of a variable speed cage machine wind generation system. *IEEE Transactions on Power Electronics*, 12(1), 87–95.
- Stol, K., Rigney, B., & Balas, M. (2000). Disturbance accommodating control of a variable-speed turbine using a symbolic dynamics structural model. In *2000 ASME Wind Energy Symposium* (p. 29).
- Stol, K. A., Balas, M. J., et al. (2003). Periodic disturbance accommodating control for blade load mitigation in wind turbines. *Transactions-American Society of Mechanical Engineers Journal of Solar Energy Engineering*, 125(4), 379–385.
- Valenciaga, F., & Puleston, P. (2008). High-order sliding control for a wind energy conversion system based on a permanent magnet synchronous generator. *IEEE Transactions on Energy Conversion*, 23(3), 860–867.
- Vu, N. T.-T., Yu, D.-Y., Choi, H. H., & Jung, J.-W. (2013). T-S fuzzy-model-based sliding-mode control for surface-mounted permanent-magnet synchronous motors considering uncertainties. *IEEE Transactions on Industrial Electronics*, 60(10), 4281–4291.
- Wang, G.-D., Wai, R.-J., & Liao, Y. (2013). Design of backstepping power control for grid-side converter of voltage source converter-based high-voltage DC wind power generation system. *IET Renewable Power Generation*, 7(2), 118–133.
- Yang, F., Li, S.-S., Wang, L., Zuo, S., & Song, Q.-W. (2014a). Adaptive backstepping control based on floating offshore high temperature superconductor generator for wind turbines. In *Abstract and applied analysis*. Hindawi Publishing Corporation.
- Yang, W., Tavner, P. J., Crabtree, C. J., Feng, Y., & Qiu, Y. (2014b). Wind turbine condition monitoring: Technical and commercial challenges. *Wind Energy*, 17(5), 673–693.
- Zhang, X., Sun, L., Zhao, K., & Sun, L. (2013). Nonlinear speed control for PMSM system using sliding-mode control and disturbance compensation techniques. *IEEE Transactions on Power Electronics*, 28(3), 1358–1365.